Engineering

Electrical Engineering fields

Okayama University *Year* 1999

Control and analysis of a unified power flow controller

Hideaki Fujita
Okayama University

Yasuhiro Watanabe
Okayama University

Hirofumi Akagi
Okayama University

Control and Analysis of a Unified Power Flow Controller

Hideaki Fujita, *Member, IEEE*, Yasuhiro Watanabe and Hirofumi Akagi, *Fellow, IEEE*
Department of Electrical Engineering, Okayama University
3-1-1 Tsushima-naka, Okayama 700-8530, Japan

Abstract - This paper presents a control scheme and comprehensive analysis for a UPFC (unified power flow controller), on the basis of theory, computer simulation and experiment. This developed theoretical analysis reveals that a conventional power-feedback control scheme makes the UPFC induce power swings in transient states. The conventional control scheme has no capability of damping power swings, so the time constant of damping is independent of active and reactive power feedback gains integrated in its control circuit. This paper proposes a generalized control scheme which is characterized by successfully damping power swings in transient states. Experimental results obtained from a 10-kVA laboratory setup agree well with both analytical and simulated results. Moreover, it is shown that the proposed control scheme is viable and effective in damping of power swings in transient states.

I. Introduction

In recent years, environment, right-of-way, and cost concerns have delayed the construction of both power stations and new transmission lines, while the demand for electronic energy has continued to grow in many countries. This situation has spurred interest in providing already existing power systems with greater operating flexibility and better utilization. The FACTS (flexible ac transmission systems) concept [1], based on applying leading edge power electronics technology to existing ac transmission systems, improves stability to increase usable power transmission capacity to its thermal limit. A UPFC (unified power flow controller) [1]-[7], which is one of the most promising devices in the FACTS concept, has the potential of power flow control and/or voltage stability in power transmission systems.

Little literature has been published on theoretical analysis in transient states, although not only feasibility studies but also practical implementation of the UPFC are presently under way. Undeland, et. al., have proposed a control scheme for the UPFC, with the focus on dynamic as well as static performance [4]. This control scheme, named "cross-coupling control," adjusts the q-axis voltage v_q to control the d-axis current i_d and the d-axis voltage v_d to control the q-axis current i_q. Computer simulation and experimental results with emphasis on dynamic performance have been shown in [4], but theoretical analysis would not be enough to support the experimental results.

This paper presents a control scheme and comprehensive analysis for a UPFC on the basis of theory, computer simulation and experiment. This developed theoretical analysis reveals that a conventional power-feedback control scheme makes the UPFC induce power swings in transient states. The conventional power-feedback control scheme has no capability of damping power swings, so the time constant of damping is independent of active and reactive power feedback gains integrated in its control circuit. This paper proposes a generalized control scheme which is characterized by successfully damping power swings in transient states. The proposed control scheme makes the UPFC act as a "damping resistance" against power swings in transient states. This stems from the concept that the series active filter proposed in [8] has the function of harmonic damping. Experimental results obtained from a 10-kVA laboratory setup agree with both analytical and simulated results. Moreover, it is shown that the proposed control scheme is viable and effective in damping power swings in transient states.

II. Basic Configuration of a UPFC

Fig. 1 shows a basic configuration of a UPFC, which is installed between the sending-end V_S and the receiving-end V_R. The UPFC consists of a combination of a series device and a shunt device, the dc terminals of which are connected to a common dc link capacitor. The series device acts as a controllable voltage source V_C, whereas the shunt device acts as a controllable current source I_C. The main purpose of the shunt device is to regulate the dc link voltage by adjusting the amount of active power drawn from the transmission line. In addition, the shunt device has the capability of controlling reactive power. In the following discussion, the shunt device is disregarded because the current flowing into the shunt device, I_C is not as large

0-7803-4489-8/98/$10.00 © 1998 IEEE

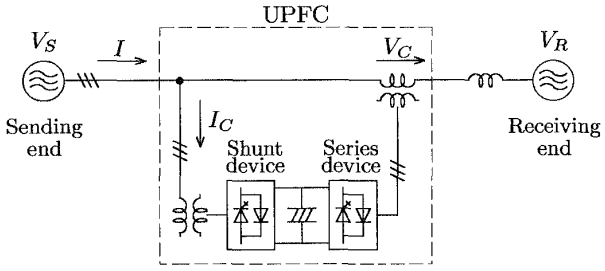

Figure 1: Basic configuration of a UPFC.

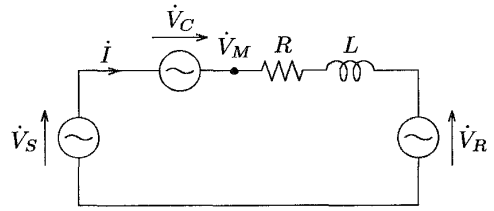

Figure 2: Single-phase equivalent circuit.

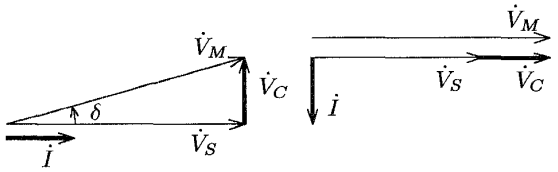

(a) Active power control. (b) Reactive power control.

Figure 3: Phaser diagrams in case of active and reactive power control.

as the transmission line current I.

Fig. 2 shows a single-phase equivalent circuit of the UPFC, where the reactor L and the resistor R represent inductance and resistance in the transmission line, respectively. It is reasonable to remove the line resistance R from Fig. 2 because $\omega_0 L \gg R$ in the overhead transmission line. Thus, the line current phaser vector, $\dot{I}$ is given by

$$\dot{I} = \frac{\dot{V}_S - \dot{V}_R + \dot{V}_C}{j\omega_0 L}. \tag{1}$$

For the sake of simplicity, the assumption of $\dot{V}_S = \dot{V}_R$ leads to the phaser diagrams shown in Fig. 3. When the output voltage $\dot{V}_C$ leads by 90° with respect to $\dot{V}_S$, $\dot{I}$ is in phase with $\dot{V}_S$, as shown in Fig. 3(a). This results in active power flow from $\dot{V}_S$ to $\dot{V}_R$. Controlling $\dot{V}_C$ to be in phase with $\dot{V}_S$ makes $\dot{I}$ lag by 90° with respect to $\dot{V}_S$, thus resulting in reactive power flow, as shown in Fig. 3(b). Since the phaser vectors are applied, the above discussion is not applicable to analysis of the dynamic behavior.

III. Conventional Control Schemes

A. *Phase-angle control*

Adjusting the amplitude of the 90° leading or lagging output voltage makes it possible to control active power. On the d-q frame coordinates based on space vectors, the d-axis current i_d corresponds to active power, and so it can be controlled by the q-axis voltage v_{Cq}. Therefore, the reference voltage vector $\boldsymbol{v}_C^* = [v_{Cd}^*, v_{Cq}^*]^t$ for the series device is given by

$$\begin{bmatrix} v_{Cd}^* \\ v_{Cq}^* \end{bmatrix} = \begin{bmatrix} 0 & 0 \\ K_p & 0 \end{bmatrix} \begin{bmatrix} i_d^* - i_d \\ i_q^* - i_q \end{bmatrix}, \tag{2}$$

where K_p [V/A] is an active power feedback gain, and i_d^* and i_q^* are active and reactive reference currents, respectively. Then the phase angle between $\dot{V}_M$ and $\dot{V}_S$, δ can be controlled by V_{Cq} as follows:

$$\delta = \tan^{-1}\left(\frac{V_{Cq}}{V_S}\right).$$

Thus, this control scheme is identical with the so-called "phase-angle control" which is one of the most basic control schemes for the UPFC.

B. *Cross-coupling control*

The "cross-coupling control" proposed in [4] has not only an active power feedback loop but also a reactive power feedback loop. This control scheme is characterized by controlling both the magnitude of $\dot{V}_M$ and the phase angle δ. As a result, the cross-coupling control enables us to achieve both active and reactive power control. On the d-q frame coordinates, the q-axis current i_q corresponds to reactive power and so it can be controlled by v_{Cd}. Therefore, the reference voltage vector of the series device is given by

$$\begin{bmatrix} v_{Cd}^* \\ v_{Cq}^* \end{bmatrix} = \begin{bmatrix} 0 & -K_q \\ K_p & 0 \end{bmatrix} \begin{bmatrix} i_d^* - i_d \\ i_q^* - i_q \end{bmatrix}, \tag{3}$$

where K_q [V/A] is a reactive power feedback gain.

The phase-angle and cross-coupling control schemes appear to be based on space vectors. However, both control schemes may not render good dynamic performance, because their control concept comes not from space vectors but from phaser vectors. The series device injects a q-axis voltage to control the d-axis current or the active power in both control schemes. The q-axis voltage, however, induces the q-axis current to flow in transient state. Therefore, the active power flow control is accompanied by

the reactive power flow control even though either control scheme provides instantaneous voltage references.

IV. Generalized Control Scheme and Transient Analysis

A. *Generalized Control Scheme*

This paper proposes a "generalized control scheme." The reference voltage vector for the series device, $\boldsymbol{v}_C^*$ is generalized, as follows:

$$\begin{bmatrix} v_{Cd}^* \\ v_{Cq}^* \end{bmatrix} = \begin{bmatrix} K_r & -K_q \\ K_p & K_r \end{bmatrix} \begin{bmatrix} i_d^* - i_d \\ i_q^* - i_q \end{bmatrix}. \tag{4}$$

Note that the proposed control scheme comprehends the phase-angle and cross-coupling control schemes, so that the proposed control scheme can be considered a generalized control scheme for the UPFC. The scheme has two additional terms with a gain K_r. A voltage vector produced by the two terms is in phase with the current error vector $\boldsymbol{i}^* - \boldsymbol{i}$. This means that the UPFC acts as a damping resistor against power swings.

B. *Transient analysis*

The following assumptions are made in transient analysis:

1. The sending-end voltage v_S is equal to the receiving-end voltage v_R, and they are three-phase balanced sinusoidal voltage sources.
2. The series device is assumed to be an ideal controllable voltage source. Therefore, the output voltage $\boldsymbol{v}_C$ is equal to its reference $\boldsymbol{v}_C^*$.

Invoking the first assumption yields $\boldsymbol{v}_S$ as follows:

$$\begin{bmatrix} v_{Su} \\ v_{Sv} \\ v_{Sw} \end{bmatrix} = \sqrt{\frac{2}{3}} V_S \begin{bmatrix} \cos\omega_0 t \\ \cos(\omega_0 t - 2\pi/3) \\ \cos(\omega_0 t + 2\pi/3) \end{bmatrix}, \tag{5}$$

where V_S is an rms voltage at the sending-end, and ω_0 is a supply angular frequency. The equivalent circuit shown in Fig. 2 provides the following equation:

$$\left(R + L\frac{d}{dt}\right) \begin{bmatrix} i_u \\ i_v \\ i_w \end{bmatrix} = \begin{bmatrix} v_{Cu} \\ v_{Cv} \\ v_{Cw} \end{bmatrix}. \tag{6}$$

Applying the d-q transformation to (5) and (6) leads to

$$\begin{bmatrix} v_{Sd} \\ v_{Sq} \end{bmatrix} = \begin{bmatrix} V_S \\ 0 \end{bmatrix}, \tag{7}$$

$$\begin{bmatrix} R + L\frac{d}{dt} & -\omega_0 L \\ \omega_0 L & R + L\frac{d}{dt} \end{bmatrix} \begin{bmatrix} i_d \\ i_q \end{bmatrix} = \begin{bmatrix} v_{Cd} \\ v_{Cq} \end{bmatrix}. \tag{8}$$

The instantaneous active and reactive powers [9], p and q are given by

$$\begin{bmatrix} p \\ q \end{bmatrix} = \begin{bmatrix} v_{Sd} \cdot i_d + v_{Sq} \cdot i_q \\ v_{Sd} \cdot i_q - v_{Sq} \cdot i_d \end{bmatrix} = V_S \begin{bmatrix} i_d \\ i_q \end{bmatrix}. \tag{9}$$

Substituting (4) for (8), along with invoking the second assumption, gives the following equation:

$$\begin{bmatrix} R + K_r + L\frac{d}{dt} & -(\omega_0 L + K_q) \\ \omega_0 L + K_p & R + K_r + L\frac{d}{dt} \end{bmatrix} \begin{bmatrix} i_d \\ i_q \end{bmatrix} = \begin{bmatrix} K_r i_d^* - K_q i_q^* \\ K_p i_d^* + K_r i_q^* \end{bmatrix}. \tag{10}$$

The Laplace functions for the active and reactive powers produce $I_d(s)$ and $I_q(s)$ as follows:

$$I_d(s) = \frac{(K_r L s + \mathrm{A}_1) I_d^* - (K_q L s + \mathrm{A}_2) I_q^*}{L^2\left(s^2 + \frac{2(K_r+R)}{L} s + \omega_n^2\right)}, \tag{11}$$

$$I_q(s) = \frac{(K_p L s + \mathrm{A}_3) I_d^* + (K_r L s + \mathrm{A}_4) I_q^*}{L^2\left(s^2 + \frac{2(K_r+R)}{L} s + \omega_n^2\right)}, \tag{12}$$

where

$$\begin{aligned} \mathrm{A}_1 &= K_p(\omega_0 L + K_q) + K_r(R + K_r), \\ \mathrm{A}_2 &= K_q R - K_r \omega_0 L, \\ \mathrm{A}_3 &= K_p R - K_r \omega_0 L, \\ \mathrm{A}_4 &= K_q(\omega_0 L + K_p) + K_r(R + K_r), \\ \omega_n &= \frac{\sqrt{(\omega_0 L + K_p)(\omega_0 L + K_q) + (K_r + R)^2}}{L}. \end{aligned}$$

Here, ω_n is an undamped natural frequency. Equations (11) and (12) conclude that the UPFC exhibits a second-order system, thus causing power swings in transient states. Damping factor ζ and power swing frequency ω are given as follows:

$$\zeta = \frac{K_r + R}{\sqrt{(\omega_0 L + K_p)(\omega_0 L + K_q) + (K_r + R)^2}}. \tag{13}$$

$$\begin{aligned} \omega &= \omega_n \sqrt{1 - \zeta^2} \\ &= \frac{\sqrt{(\omega_0 L + K_p)(\omega_0 L + K_q)}}{L}, \end{aligned} \tag{14}$$

Equation (13) tells us that the larger the gain K_r, the closer ζ is to unity. Equation (14) leads to the fact that the larger the power feedback gains K_p and K_q, the larger the power swing frequency ω. The time constant of damping of power swings, τ is given by

$$\tau = \frac{1}{\zeta \omega_n} = \frac{L}{K_r + R}. \tag{15}$$

Note that K_r acts as a damping resistor. Therefore, increasing K_r reduces the time constant and improves the transient stability. The phase-angle control and cross-coupling control schemes have no capability of damping power swings because $K_r = 0$.

V. Experimental System Configuration

A. *Main circuit*

Fig. 4 and Table 1 show a main circuit of an experimental system rated at 10 kVA and its circuit parameters. The main circuit of the series device consists of three single-phase H-bridge voltage-fed PWM inverters rated at 1.5 kVA. A PWM control circuit compares reference voltage v_C^* with a triangle carrier signal of $f_{SW} = 1$ kHz in order to generate twelve gate signals. An equivalent switching frequency is 2 kHz, which is twice as high as f_{SW} because three H-bridge PWM inverters are used. A three-phase diode rectifier is employed as the shunt device. A reactor L and a resistor R, representing the impedance of the transmission line, are inserted between v_S and v_R.

In the experimental system, v_S and v_R are connected to a common power supply v. Thus, no power flow occurs as long as the series device is not operated. The series device always delivers a small amount of active power to the transmission line, which equals the power loss dissipated in the resistor R. A three-phase PWM converter should be employed in a practical system because the magnitude and phase of v_S may differ from those of v_R. While the series device draws active power from the transmission line, the shunt device should regenerate the active power via the dc link capacitor to the transmission line.

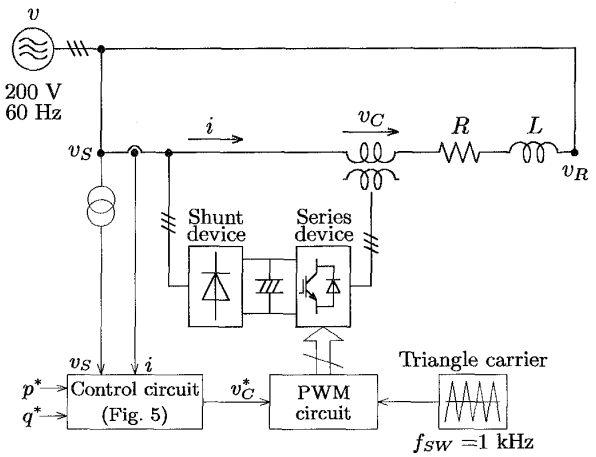

Figure 4: Main circuit of an experimental system.

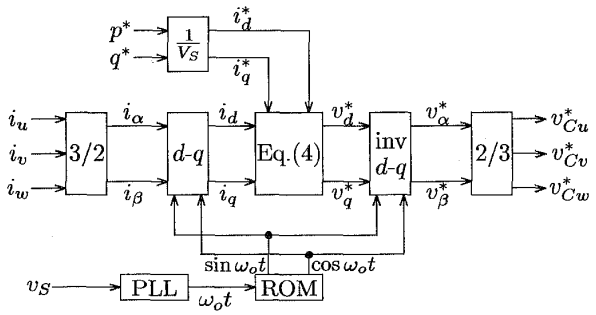

Figure 5: Control circuit.

B. *Control circuit*

Fig. 5 shows a block diagram of the control circuit. The three- to two-phase transformation obtains i_α and i_β from the three-phase currents i_u, i_v and i_w. The d-q transformation gets i_d and i_q from i_α and i_β with the help of sinusoidal signals of $\sin\omega_0 t$ and $\cos\omega_0 t$ taken from a read only memory (ROM). The phase information $\omega_0 t$ is generated by a phase-lock-loop (PLL) circuit. Then v_d^* and v_q^* are given by (4).

The power feedback gains are set to $K_p = K_q = 0.5$ V/A in the following experiments. From (13), the feedback gain K_r is obtained as

$$K_r = \frac{\zeta\sqrt{(\omega_0 L + K_p)(\omega_0 L + K_q)}}{\sqrt{1-\zeta^2}} - R. \tag{16}$$

In order to get a damping factor of $\zeta = 0.8$, K_r should be designed as

$$\begin{aligned} K_r &= \frac{0.8\sqrt{(2\pi \times 60 \times 0.001 + 0.5)^2}}{\sqrt{1-0.8^2}} - 0.04 \\ &= 1.13 \text{ V/A}. \end{aligned}$$

In the experimental system, therefore, gain K_r is set to 1.2 V/A.

Table 1: Experimental system parameters.

Controllable power rating	P	10 kW
Series device capacity	P_{INV}	1.5 kVA (=15%)
Peak voltage of v_C	V_{CP}	±17 V (=15%)
Utility line-to-line voltage	V	200 V
Utility angular frequency	ω_0	$2\pi \times 60$ rad/s
Line inductance	L	1.0 mH (=10%)
Line resistance	R	0.04 Ω (=1%)

(200 V, 10 kVA, 60 Hz base)

VI. Simulated and Experimental Results

Figs. 6 - 9 show simulated and experimental waveforms for a step change in the active power reference p^*. Table 2 shows experimental and theoretical values of damping factor ζ, power swing frequency ω and damping time constant τ. The experimental waveforms of the series device voltage v_C are measured through a low pass filter with a cut-off

Table 2: Experimental and theoretical values of damping factor ζ, power swing frequency ω and damping time constant τ.

(a) Experimental values.

Control Schemes	ζ	ω [rad/s]	τ [ms]
phase-angle control	0.067	520	28
cross-coupling control	0.053	740	26
proposed control (Fig.8)	0.76	900	0.95

(b) Theoretical values.

Control Schemes	ζ	ω [rad/s]	τ [ms]
phase-angle control	0.069	570	25
cross-coupling control	0.046	880	25
proposed control	0.82	880	0.81

frequency of 400 Hz because the switching frequency of the series device is 1 kHz. Circuit simulation software based on PSpice is used to calculate the following simulated results. The series device is assumed to be an ideal controllable voltage source which is equal to the reference voltage v_C^* in this simulation. The simulated and experimental waveforms agree well with each other not only in the steady state but also in the transient state.

Fig. 6 shows waveforms in the case of the phase-angle control scheme. Non-negligible power swing with a frequency of 520 rad/s occurs in the waveforms of p and q. After the step change, p and q reach their final values in 70 ms. Equation (15) determines the theoretical time constant

$$\tau = \frac{L}{K_r + R} = \frac{1.0\,\text{mH}}{0 + 0.04\,\Omega} = 25\,\text{ms},$$

which agrees well with the experimental value in Table 2(a).

Fig. 7 shows waveforms in the case of the cross-coupling control scheme. It is clear from (14) that addition of the reactive power feedback gain K_q increases the power swing frequency ω from 520 rad/s to 740 rad/s. Since (15) shows that the time constant τ is independent of K_p and K_q, it takes the same time as that in Fig. 6 for p and q to reach their steady-state values.

Fig. 8 shows waveforms in the case of the proposed control scheme. No power swing occurs in p and q. From (15), the theoretical time constant is

$$\tau = \frac{L}{K_r + R} = \frac{1.0\,\text{mH}}{1.2 + 0.04\,\Omega} = 0.81\,\text{ms},$$

which is superior to that of the conventional control schemes. The proposed control scheme has the capability of damping power swings and improving transient characteristics. However, significant steady-state errors exist in p and q because K_p and K_q include no integral gain.

Fig. 9 shows waveforms in the case of the proposed control scheme with proportional and integral (PI) gains for K_p and K_q. The integral gain is set to $T_I = 5$ ms, so that the steady-state errors are removed from p and q. Note that addition of the integral gain has no effect on damping of power swings.

VII. Conclusion

This paper has proposed a generalized control scheme for the UPFC, along with a comprehensive analysis. The experimental results obtained from the laboratory system rated at 10 kVA has shown concurrence with analytical ones. This paper has revealed the following essentials:

- Conventional power-feedback control schemes make the UPFC induce power swings in transient states.
- The time constant of damping is independent of the active and reactive power feedback gains K_q and K_q. Therefore, the conventional control schemes based on only the power feedback loops are not capable of damping power swings.
- The feedback gain K_r with a physical meaning of a resistor is effective in damping of power swings.
- The proposed control scheme achieves a quick response of active and reactive power without causing power swings and producing steady-state errors.

References

[1] L. Gyugyi, "Unified Power-Flow Control Concept for Flexible AC Transmission Systems," IEE Proceedings-C, Vol.139, pp.323-331, July, 1992

[2] B. T. Ooi, S. Z. Dai, X. Wang, "Solid-State Series Capacitive Reactance Compensators," *IEEE Trans. on Power Delivery*, Vol.7, No.2, pp.914-919, 1990

[3] B. S. Rigby, R. G. Harly, "An Improved Control Scheme for a Series Capacitive Reactance Compensator Based on a Voltage Source Inverter," *IEEE/IAS Annual Meeting*, pp.870-877, 1996

[4] Q. Yu, S. D. Round, L. E. Norum, T. M. Undeland, "Dynamic Control of a Unified Power Flow Controller," IEEE PESC '96, pp.508-514, 1996

[5] L. Gyugyi, C. D. Schauder, K. K. Sen, "Static Synchronous Series Compensator:A Solid-State Approach to the Series Compensation of Transmission Lines," *IEEE Trans. on Power Delivery*, Vol.12, No.1, pp.406-413, 1997

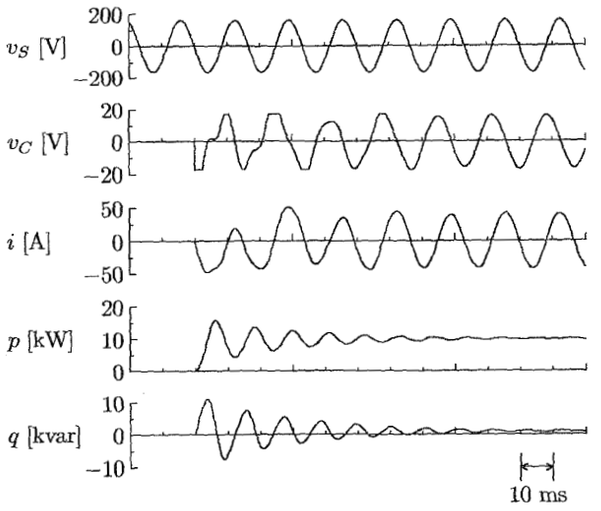

(a) Simulated waveforms.

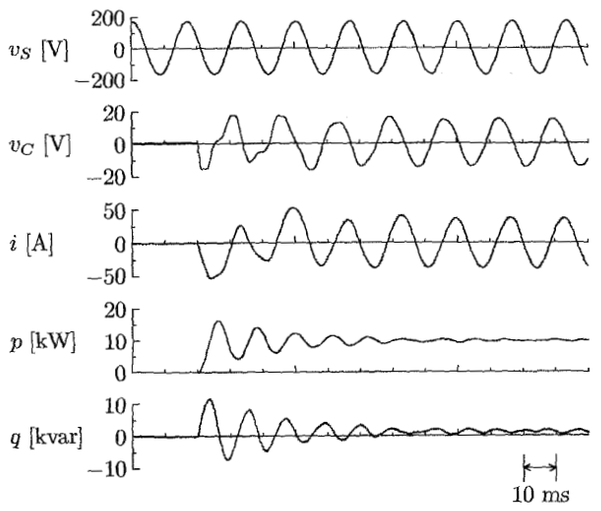

(b) Experimental waveforms.

Figure 6: Simulated and experimental waveforms when the phase-angle control scheme is applied. (K_p = 0.5 V/A, p^* = 16.5 kW)

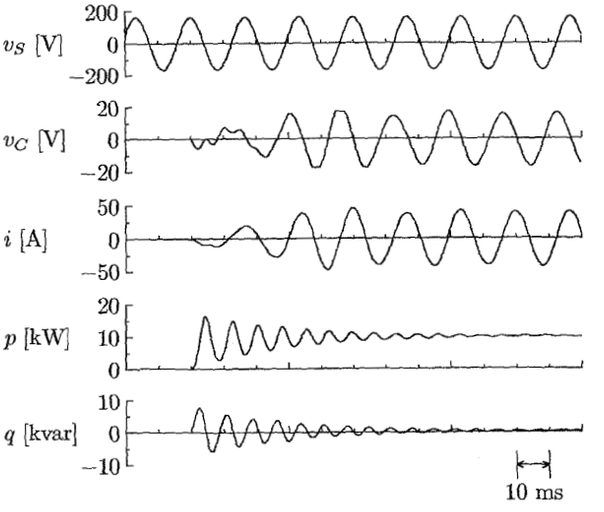

(a) Simulated waveforms.

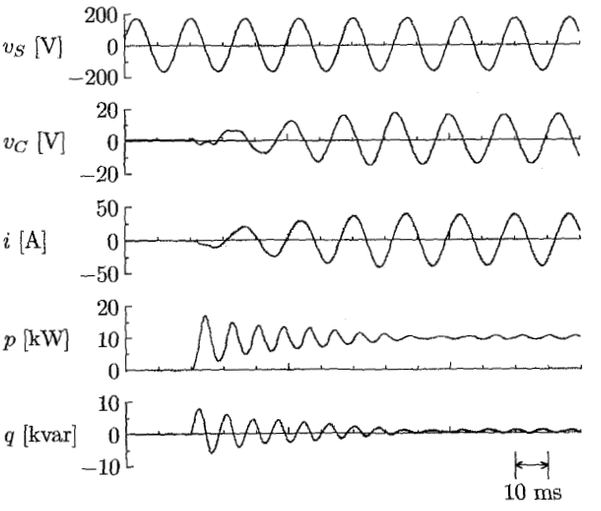

(b) Experimental waveforms.

Figure 7: Simulated and experimental waveforms when the cross-coupling control scheme is applied. ($K_p = K_q$ = 0.5 V/A, p^* = 16.5 kW, $q^* = 0$)

[6] Y. Jiang, A. Ekstrom, "Optimal Controller for the Combination System of a UPFC and Conventional Series Capacitors," EPE'97 Vol.1, pp.372-337, 1997

[7] Y. Chen, B. Mwinyiwiwa, Z. Wolanski, B. T. Ooi, "Unified Power Flow Controller (UPFC) Based on Chopper Stabilized Multilevel Converter," IEEE PESC '97, pp.331-337, 1997

[8] F. Z. Peng, H. Akagi and A. Nabae, "A New Approach to Harmonic Compensation in Power Systems –A Combined System of Shunt Passive and Series Active Filters," *IEEE Trans. on IAS*, Vol. 26, No. 6, pp. 983-990, 1990

[9] H. Akagi, Y. Kanazawa and A. Nabae, "Instantaneous reactive power compensators comprising switching devices without energy storage components," *IEEE Trans. on IAS*, Vol. 20, No. 3, pp. 625-630, 1984

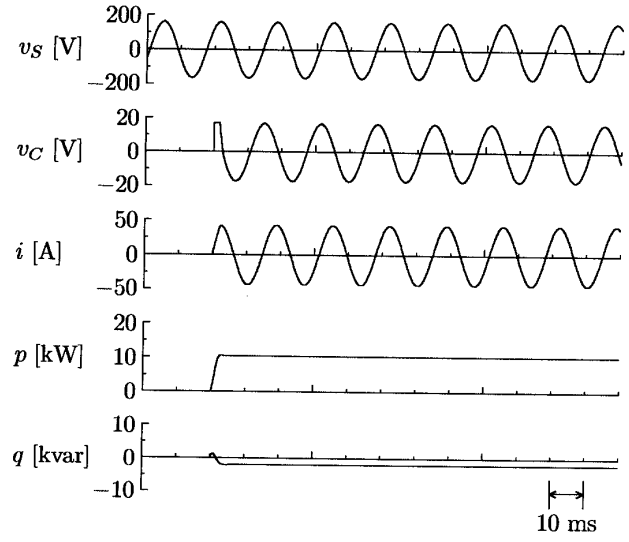

(a) Simulated waveforms.

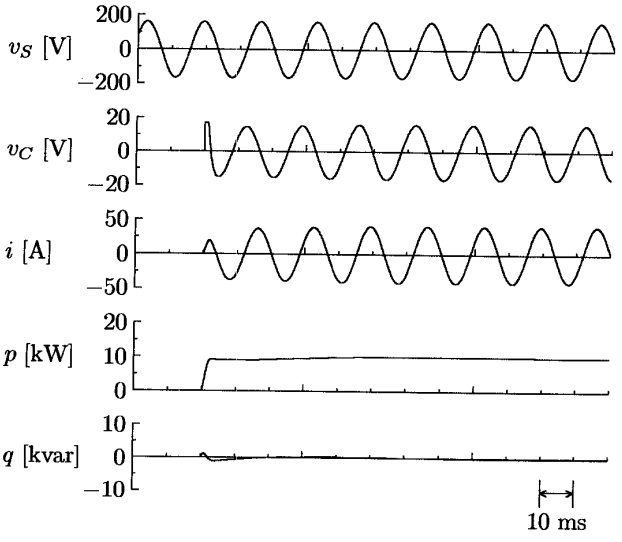

(a) Simulated waveforms.

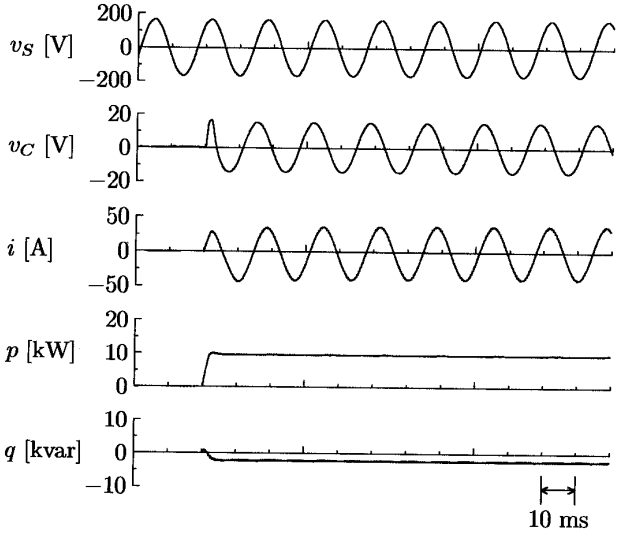

(b) Experimental waveforms.

Figure 8: Simulated and experimental waveforms when the proposed control scheme with P gain is applied. ($K_p = K_q = 0.5$ V/A, $K_r = 1.2$ V/A, $p^* = 14.5$ kW, $q^* = 0$)

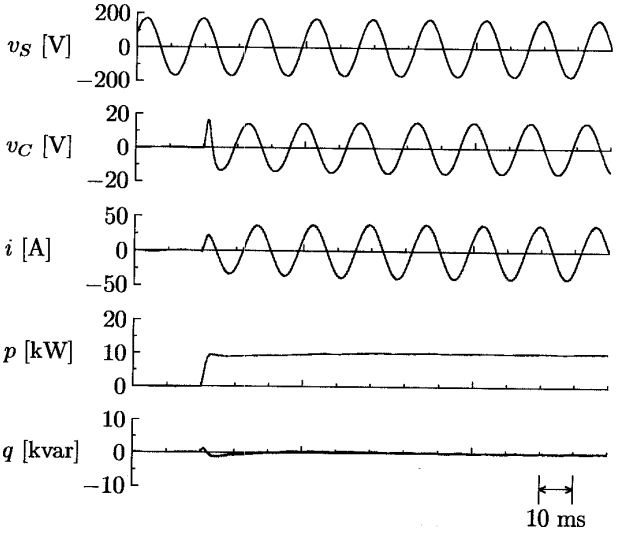

(b) Experimental waveforms.

Figure 9: Simulated and experimental waveforms when the proposed control scheme with PI gain is applied. ($K_p = K_q = 0.5$ V/A, $K_r = 1.2$ V/A, $T_I = 5$ ms, $p^* = 10$ kW, $q^* = 0$)